RSC Advances

PAPER

View Article Online
View Journal | View Issue

Cite this: *RSC Adv.*, 2020, **10**, 23276

Arginine–glycine–aspartate (RGD)-targeted positron-labeled dendritic polylysine nanoprobe for tumor PET imaging

Qi Fang,†[a] Yongcheng Xiao,†[b] Rongqin Zhang,[c] Jilin Yin,[c] Deming Xie*[b] and Xinlu Wang *[a]

This work investigated the optimization of the ^{68}Ga radiolabeling of the dendritic polylysine-1,4,7-triazacyclononane-1,4,7-triacetic acid conjugate (DGL-NOTA). Under pH = 4.0, reaction temperature of 70 °C, and incubation time of 10.0 min, the conjugate (DGL-NOTA) radiochemical yield was between 50% and 70%. After separation and purification, the radiochemical purity was greater than 98%. The radiolabeled formulation (^{68}Ga-NOTA-DGL-PEG-RGDyC) remained stable in both phosphate buffer and serum (all radiochemically greater than 95%) for up to 2 hours with a specific activity of 30 GBq/μmol. Cellular experimental studies have shown that radiolabeled preparations can rapidly enter U87MG cells, and after 2 hours, there was still retention of imaging agents in the cells. *In vivo* distribution studies had shown that the tracer is excreted by the kidneys. Two hours after injecting the imaging agent, the U87MG tumor tissue uptake value was (4.67 ± 0.09)% ID/g. Positron emission tomography (PET) imaging in animals showed that ^{68}Ga-NOTA-DGL-PEG-RGDyC had good targeting and can be enriched in tumor sites. Through hemolysis testing and morphological changes of red blood cells, it was proved that NOTA-DGL-PEG-RGDyC has good blood compatibility.

Received 27th March 2020
Accepted 2nd June 2020

DOI: 10.1039/d0ra02813d

rsc.li/rsc-advances

1. Introduction

Malignant tumors now pose a serious threat to public health worldwide. The National Cancer Institute believes that proper tumor screening can prevent 3% to 35% of cancer patients from dying early in the disease, and tumor screening may reduce the mortality of some tumors. Conventional imaging examinations (B-ultrasound,[1] CT,[2] and magnetic resonance imaging[3]) can only achieve imaging analysis and judgment on lesions, which cannot be accurately diagnosed at an early stage, and have certain limitations.[4] Positron emission computed tomography (PET/CT) technology is one of the rapidly developing technologies in the field of medical imaging. It has metabolic imaging capabilities, which can be used to observe and characterize biochemical and physiological abnormalities, such as over-expression of receptors, and in the disease. Make non-invasive real-time measurements before macroanatomical features appear.[5,6] Among the radionuclides used in PET clinical practice, ^{68}Ga has a suitable half-life, $t_{1/2}$ = 67.7 min, which is convenient to prepare, short in reaction time and high in radiochemical yield (RCY). The removal rate in the blood is faster, and it has become the focus of positron emission labeling research.[7–9] For example, ^{68}Ga-NOTA-TOC could detect more lesions than other imaging agents;[10] while ^{68}Ga-NOTA-TATE could not only identify the primary tumor, but also the detection of metastases was of great significance.[11] In addition to labeling somatostatin analogues (SSTA), ^{68}Ga had a certain diagnostic value for labeling melanocyte stimulating hormone.[12]

However, currently used imaging agents are not targeted, so it is particularly important to find an imaging agent that has good targeting properties for tumor tissues. Vascular endothelial growth factor (VEGF) receptors and integrin αvβ3 receptors are ideal targets for tumor tissues. Integrin αvβ3 is highly expressed on the surface of tumor neovascular endothelial cells and on the surface of some tumor cells, but not expressed or low expressed in normal tissue.[13] Integrin αvβ3 mediates signal transduction between cells and cells and extracellular matrix. Using this feature can achieve effective brain transport. Among them, the most widely used is the arginine–glycine–aspartate sequence (RGD) application. RGD peptides are a class of short peptides, and they exist in organisms and play a key role in tumor angiogenesis, metastasis and growth. RGD peptides, especially RGDyC, have specific binding ability to integrin αvβ3 on neovascular endothelial cells.[14,15] Yi Yang *et al.*[16] modified nano-gold and successfully synthesized RGDyC@AuNPs-Gd^{99} mTc. Through *in vitro* and *in vivo* experiments, the nanoprobe proved to be highly specific for integrin αvβ3 positive cells and

[a]*Department of Nuclear Medicine, The First Clinical Hospital of Guangzhou Medical University, Guangzhou 510120, China. E-mail: 71Lu@163.com*

[b]*Key Laboratory of Biomaterials of Guangdong Higher Education Institutes, Guangdong Provincial Engineering and Technological Research Center for Drug Carrier Development, Department of Biomedical Engineering, Jinan University, Guangzhou 510632, China. E-mail: bme2004@126.com*

[c]*Department of Nuclear Medicine, General Hospital of Southern Theater Command, PLA, Guangzhou 510010, China*

† These authors contributed equally to this work.

tumor tissue. *In vivo* and *in vitro* experiments, the higher concentration of nanoprobes in tumor cells or tumor tissues can be seen, which has great potential in tumor imaging and radiotherapy. In recent years, the technology of targeted nano drug delivery systems has developed rapidly. Accurate targeting of tumor tissues and cells minimizes the toxic side effects of normal cell, tissue and organ function. Nanoparticles have enhanced permeability[17] and enhanced permeability and retention (EPR) effect,[18] so they are more likely to accumulate in tumor tissue and enter the tumor cells across the cell membrane.

Dendrimers are a class of nanoscale synthetic polymers with a well-defined composition and a regular branched dendritic structure produced by stepwise growth,[19] which can exhibit an "EPR" effect in targeted therapy/drug delivery methods.[20,21] Polyamide-amine (PAMAM) dendrimers are early dendrimers. However, PAMAM at the amino terminus has hemolytic toxicity and cytotoxicity, so its application *in vivo* is limited.[22] Compared with PAMAM, dendrigraft poly-L-lysines (DGL) has good biocompatibility,[23] antibacterial,[24] no immunogenicity,[25] and low toxicity.[23] These properties make DGL an emerging role in a variety of biomedical applications[22] These applications include use as a drug carrier,[26] gene delivery,[27,28] and imaging diagnosis.[29–31] The large amount of amino groups on the surface of DGL can be chemically reacted with α-malemidyl-ω-*N*-hydroxysuccinimidyl polyethyleneglycol (NHS-PEG-MAL), and the MAL group at the DGL-PEG end can be reacted with a polypeptide containing a cysteine group to facilitate chemical modification. The surface is operatively linked to the targeted head base to achieve the goal of targeting tumor tissue.[32]

In this manuscript, a triazacyclononane triacetate monoester (NOTA-NHS) was coupled to a DGL dendrimer. Nano-targeting probe ^{68}Ga-NOTA-DGL-PEG-RGDyC was constructed by coupling dendritic polylysine-triazacyclononane triacetic acid (NOTA-DGL) with the targeting polypeptide arginine–glycine–aspartic acid–D-tyrosine–cysteine (RGDyC) using NHS-PEG-MAL as a coupling agent. The prepared nano-probes were studied *in vitro* using U87 cells as target cells. Pre-clinical evaluation of the ^{68}Ga labeled product was performed by *in vitro* experiments, cytotoxicity, animal distribution, and imaging studies.

2. Experimental section

2.1. Materials

Dendrigraft poly-L-lysine (DGL) [generation = 3, containing 123 primary amino groups] was purchased from Colcom, France. Double antibody, fetal bovine serum (FBS), and trypsin-ethylenediaminetetraacetic acid (0.25%) were from Gibco (BRL, MD). α-malemidyl-ω-*N*-hydroxysuccinimidyl polyethyleneglycol (NHS-PEG-MAL, MW 2000) was obtained from Beijing Keykai Technology Co., Ltd. Arginine–glycine–aspartic acid–D-tyrosine–cysteine (RGDyC) was purchased from Jill Biochemical Co., Ltd (Shanghai, China). Dimethyl sulphoxide (DMSO), sodium acetate and glacial acetic acid were obtained from Bailingwei Chemical Technology Co., Ltd (Shanghai, China). NOTA-NHS was bought from CHEMATECH. Ethanol and hydrochloric acid were purchased from Da Mao Chemical Reagent Factory. ^{68}Ga was gained from a ^{68}Ge/^{68}Ga generator (ITG, Munich, Germany) and eluted using 0.05 M HCl. PD-10 column was obtained from GE Healthcare Life Sciences (NJ, USA). The radiochemical purity of the ^{68}Ga-NOTA-DGL-PEG-RGDyC dendrimers was determined by Radio-TLC (Shimadzu, Japan). PET images were recorded on a Siemens Inveon small-animal PET scanner (Siemens, Germany) with a typical acquisition time of 2 h.

2.2. Synthesis of DGL-PEG-RGDyC

20 mg of NHS-PEG-MAL and 2 mg of RGDyC were dissolved in 1 mL sodium acetate buffer (0.1 M pH = 6.0), and the reaction was stirred at room temperature for 5 min in the dark. Subsequently, 5 mg DGL-G_3 was dissolved in 500 μL boric acid buffer (0.05 M pH 9.0) and mixed with the above reaction liquid. The mixed system was stirred at room temperature for 14 h in the dark. After the end of the reaction, the pH of the system was adjusted to 7.0 and excess β-mercaptoethanol was added to remove unreacted MAL groups. After 2 hours of reaction, unreacted NHS-PEG-MAL and RGDyC were removed by ultrafiltration (MWCO 10 000; 4500 rpm, 15 min, 8 times total).

2.3. Synthesis of NOTA-DGL-PEG-RGDyC

4.3 mg NOTA-NHS was dissolved in 5 mL anhydrous DMSO, dissolved thoroughly, and added to 5 mL of DGL-PEG-RGDyC solution. The reaction was stirred at room temperature for 24 h in the dark. After completion of the reaction, it was dialyzed against 0.5 mol L^{-1} sodium acetate buffer of pH = 4.0 (3d, 5 times total), and a NOTA-DGL-PEG-RGDyC solution having a concentration of 1 mg mL^{-1} was obtained. According to the literature,[33] the remaining amine of NOTA-DGL-PEG-RGDyC was converted to an acetyl group by reaction with acetic anhydride. Briefly, 37.7 mg of NOTA-DGL-PEG-RGDyC was dissolved in 10 mL of water, followed by adding 100 μL triethylamine and stirred under a strong magnet for 0.5 h. Then, acetic anhydride (52 μL, 5 μmol) was added dropwise to the above dendrimer/triethylamine mixture solution under vigorous magnetic stirring. After 24 hours, the mixture was treated as above mentioned procedures to give a NOTA-DGL-PEG-RGDyC dendrimer.

2.4. Preparation of ^{68}Ga-NOTA-DGL-PEG-RGDyC

The ^{68}Ge/^{68}Ga generator was rinsed with 2.5 mL 0.05 M HCl at a flow rate of 1 mL min^{-1}, and the eluate was collected, 5 pieces each for 0.5 mL. Then, the eluent was tested for activity, and the eluate with the highest activity was selected. 32.5 μL 1.0 mol L^{-1} sodium acetate solution was added to adjust the pH to 4.0–4.2. Finally, the eluate was added to 200 μL of NOTA-DGL-PEG-RGDyC sodium acetate buffer, and the reaction was stirred at 70 °C for 10 min in the dark to obtain ^{68}Ga-NOTA-DGL-PEG-RGDyC.

2.5. Characterization

Chemical structure of DGL, DGL-PEG, and DGL-PEG-RGDyC was characterized by ^{1}H NMR spectroscopy (300 MHz, Varian, USA) using deuterium oxide (D_2O) as the solvent. UV-visible spectra of NOTA, DGL-PEG-RGDyC, and NOTA-DGL-PEG-RGDyC were measured by UV 2450/2250 (Shimadzu) spectrophotometer. The particle size of NOTA-DGL and NOTA-DGL-

PEG-RGDyC were measured by dynamic light scattering laser nanoparticle size analyzer (Zetasizer Nano ZS). The measurement temperature was 25 °C.

2.6. Quality control tests of ^{68}Ga-NOTA-DGL-PEG-RGDyC

2.6.1. Identification and purification. ^{68}Ga-NOTA-DGL-PEG-RGDyC was identified by Thin Layer Chromatography (TLC) and purified by PD10 purification column. Briefly, 1 μL of the marker was spotted with 0.9% physiological saline as a developing agent. The PD10 column was equilibrated with 25 mL 0.01 mL L^{-1} PBS solution, and 500 μL of the reaction mixture was added, followed by rinsing with 5 mL 0.9% physiological saline. After the rinsing, the radioactivity of the eluent was measured, and the eluent with the highest activity was measured for radio-TLC. *In vitro* and *in vivo* biological experiments were performed when the radiochemical purity was higher than 99%.

2.6.2. Determination of physical and chemical properties. The prepared radioactive nano-molecular probe was dissolved in PBS buffer, and its color, clarity, and transparency were visually observed. A slight amount of sample was analyzed for pH using standard pH test paper.

2.6.3. Stability evaluation. The *in vitro* stability of the radiolabeled preparation was determined by measuring the radiolabeling efficiency. In detail, 20 μL (about 2.03 MBq) ^{68}Ga-NOTA-DGL-PEG-RGDyC solution was placed in 0.5 mL PBS buffer (pH = 7.4, 0.01 mol L^{-1}), and incubated at 37 °C for 30 min, 60 min, 90 min and 120 min. Subsequently, 100 μL of the solution was measured for its radiochemical purity to observe its stability in PBS buffer, which was repeated three times. The stability of the ^{68}Ga-NOTA-DGL-PEG-RGDyC solution in calf serum was measured by the same method.

2.7. Cytotoxicity

The cytotoxicity of NOTA-DGL-PEG-RGDyC, ^{68}Ga-NOTA-DGL-PEG-RGDyC and ^{68}Ga-NOTA-DGL-Ac on U87MG cells was evaluated by the method of detecting cellular activity by CCK-8. The specific steps were as follows: First, U87MG cells were seeded in a 96-well plate at a density of 5000 cells per well, and then placed in a carbon dioxide incubator for culture overnight. Subsequently, the original medium was aspirated and replaced with fresh complete medium containing different concentrations of NOTA-DGL-PEG-RGDyC. The selected NOTA-DGL-PEG-RGDyC was in the range of 0–200 μg mL^{-1}. After 24 h or 48 h of culture, the cells were washed once with PBS, and 100 μL fresh medium (containing 10% CCK-8) was added to each well. The cells were incubated in the incubator for a period of time. Finally, the absorbance at 450 nm was detected and recorded using a microplate reader. Cell viability was calculated by the following formula: cell viability (%) = (experimental absorbance − blank group absorbance)/(negative control absorbance − blank group absorbance) × 100%.

2.8. Cell uptake experiment

Cellular uptake of ^{68}Ga-NOTA-DGL-Ac with and without RGDyC functionalization was analyzed to confirm the targeting ability of RGDyC. In detail, the human glioma cell line U87MG was inoculated into a 24-well culture plate having a density of 5 × 10^4 cells per well and cultured in a humidified incubator (5% CO_2) at 37 °C for 12 hours. The old medium was removed and replaced by fresh PBS solution containing 26 KBq of ^{68}Ga-NOTA-DGL-PEG-RGDyC or ^{68}Ga-NOTA-DGL-Ac. The PBS group was used as a blank control group. After incubation at 37 °C for 20 min, 40 min, 80 min and 120 min, each well was washed 3 times with 0.5 mL of frozen PBS. The cells were then digested with 0.25% trypsin/0.02% EDTA, and the cell suspension was collected, and the radioactivity count was measured with a gamma counter. The cell uptake data was all adjusted for attenuation and expressed by the cell binding rate, which was the percentage added dose. The experiment was set up in three parallels and repeated three times.

2.9. Cell efflux experiments

The human glioma cell line U87MG was inoculated into a 24-well culture plate having a density of 5 × 10^4 cells per well and cultured in a humidified incubator (5% CO_2) at 37 °C for 12 h. The old medium was removed, and replaced by fresh PBS solution containing 185 KBq of ^{68}Ga-NOTA-DGL-PEG-RGDyC or ^{68}Ga-NOTA-DGL-Ac. After incubating at 37 °C for 1 h, the original medium was removed, washed 3 times with ice-cold PBS, and then serum-free medium was added at 37 °C for 0 min, 20 min, 40 min, 80 min and 120 min. Subsequent processing steps refered to cellular uptake.

2.10. Establishment of U87MG tumor-bearing mouse model

All animal procedures were performed in accordance with the Guidelines for Care and Use of Laboratory Animals of Guangzhou Medical University and approved by the Animal Ethics Committee of Guangzhou Medical University. Healthy BALB/C nude mice were taken from Beijing Weitong Lihua Experimental Animal Technology Co., Ltd. A tumor-bearing nude mouse model was established by subcutaneous injection of 5 × 10^6 U87MG cells. Tumor size (measured by vernier calipers) was measured every 2 days from the 3rd day after inoculation. When the tumor diameter of nude mice reached 0.8–1.0 cm, it could be used for *in vivo* biodistribution experiments and micro-PET imaging of tumor-bearing mice.

2.11. *In vivo* biological distribution of normal mice

Twelve nude mice that were fasted for 12 hours were divided into 4 groups of three. A 50–75 μL tracer was taken from the syringe and the activity was measured and injected into the nude mice through the tail vein. After the injection of the tracer for 5 min, 30 min, 60 min and 120 min, the eyeballs were taken for blood collection. Subsequently, the main organs (heart, lung, liver, spleen, kidney, stomach, intestine, pancreas, brain) of the nude mice were removed, washed with physiological saline, dried and stored in a pre-weighed test tube. The counter tube containing the organ tissue was counted by gamma counting using a gamma counter, and the radioactivity count per gram of tissue was calculated after attenuation correction, expressed as a percentage of injection per gram of tissue (% ID/g).

2.12. *In vivo* biodistribution of U87MG tumor mice

Each of the U87MG-bearing tumor mice was injected with about 1.85 MBq (50 μCi) ^{68}Ga-NOTA-DGL-PEG-RGDyC through the tail vein under 2% isoflurane anesthesia. Two hours after the injection of the imaging agent, the tumor-bearing mice were sacrificed by cervical dislocation. The tumor and main organs were dissected and separated and placed in an empty counter tube for weighing (total weight). The radioactivity count was then measured with a gamma counter, and the radioactivity uptake of tumors and normal organs was expressed in % ID/g.

2.13. Positron emission tomography (PET) imaging of tumor bearing mice

Under the 2% isoflurane anesthesia, 1.85 MBq (50 μCi) of ^{68}Ga-NOTA-DGL-PEG-RGDyC was injected into the tumor-bearing mice through the tail vein. Static images were taken after 120 min injection of the imaging agent. The radioactivity uptake value was measured and expressed in % ID/g.

2.14. Blood compatibility

2.14.1. Hemolysis assay *in vitro*. Different concentrations of NOTA-DGL-PEG-RGDyC in PBS were prepared at concentrations of 0.2 mg mL^{-1}, 0.1 mg mL^{-1}, 0.01 mg mL^{-1}, and 0 mg mL^{-1}, respectively. Deionized water and PBS were used as positive and negative control groups, respectively. 4 mL samples of each concentration were placed in a centrifuge tube and incubated with 200 μL of 16% red blood cell suspension. At a predetermined time point (1 h, 3 h, 5 h, 8 h, 18 h, and 24 h), the supernatant was collected by centrifugation at 1000×*g* for 5 min. The absorbance at 540 nm of each sample was measured, and the hemolysis rate was calculated by the following formula.[34]

$$\text{hemolysis (\%)} = (A - C)/(B - C) \times 100,$$

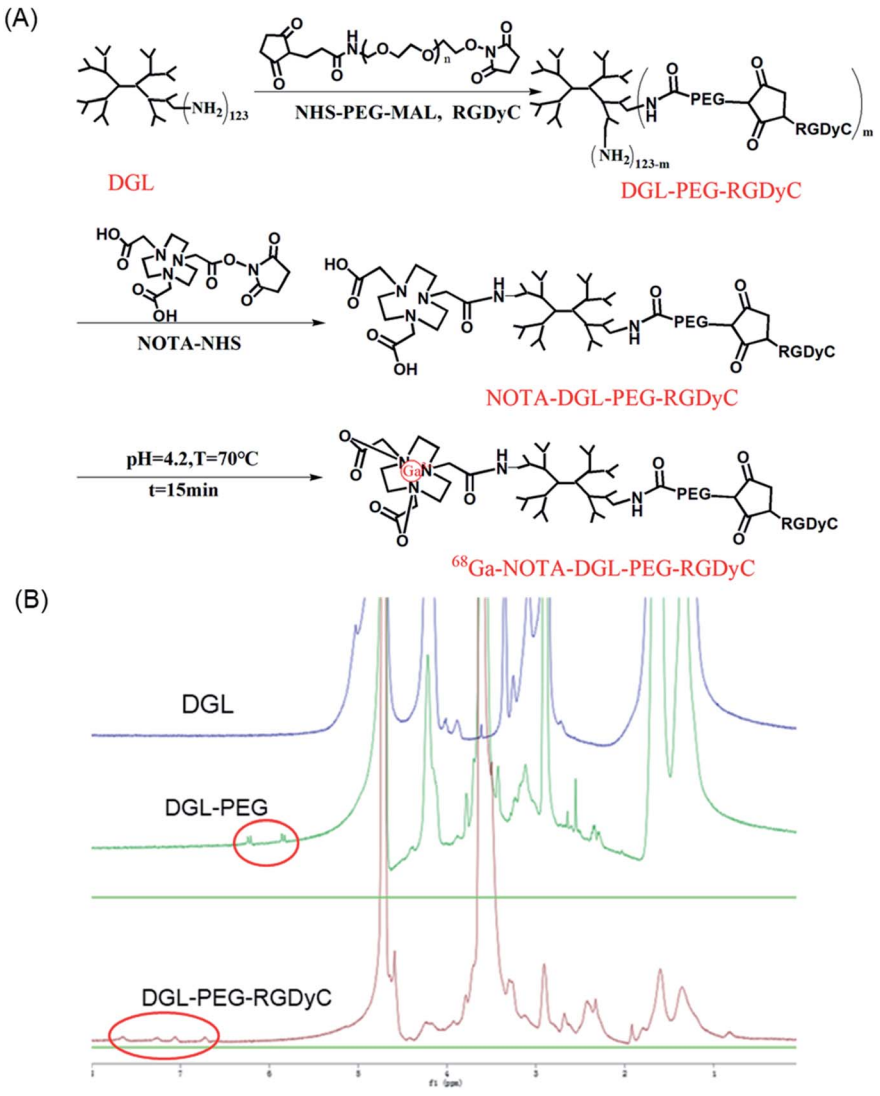

Fig. 1 (A) Schematic showing the synthesis routes to ^{68}Ga-NOTA-DGL-PEG-RGDyC. (B) ^{1}H NMR spectra for DGL, DGL-PEG and DGL-PEG-RGDyC.

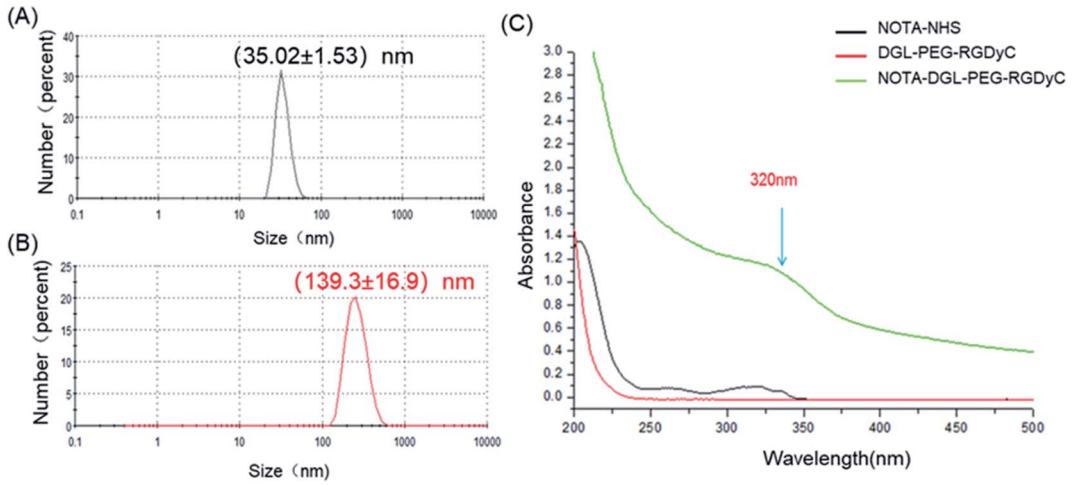

Fig. 2 Particle size distribution of (A) NOTA-DGL and (B) NOTA-DGL-PEG-RGDyC. (C) UV-Vis spectra of NOTA-NHS, DGL-PEG RGDyC and NOTA-DGL-PEG-RGDyC.

where A, B, and C represent the experimental group, the positive control group, and absorbance of the negative control group.

2.14.2. Morphology of red blood cells (RBCs). Different concentrations of NOTA-DGL-PEG-RGDyC (0.2 mg mL^{-1}, 0.1 mg mL^{-1}, and 0.01 mg mL^{-1}) were configured, and PBS was used as a negative control group. NOTA-DGL-PEG-RGDyC solution was blended with appropriate amount of red blood cells. After incubating for 1 h, the supernatant was centrifuged to collect the lower red blood cell pellet, washed with PBS, and then fixed with 4% paraformaldehyde. After the samples to be treated were

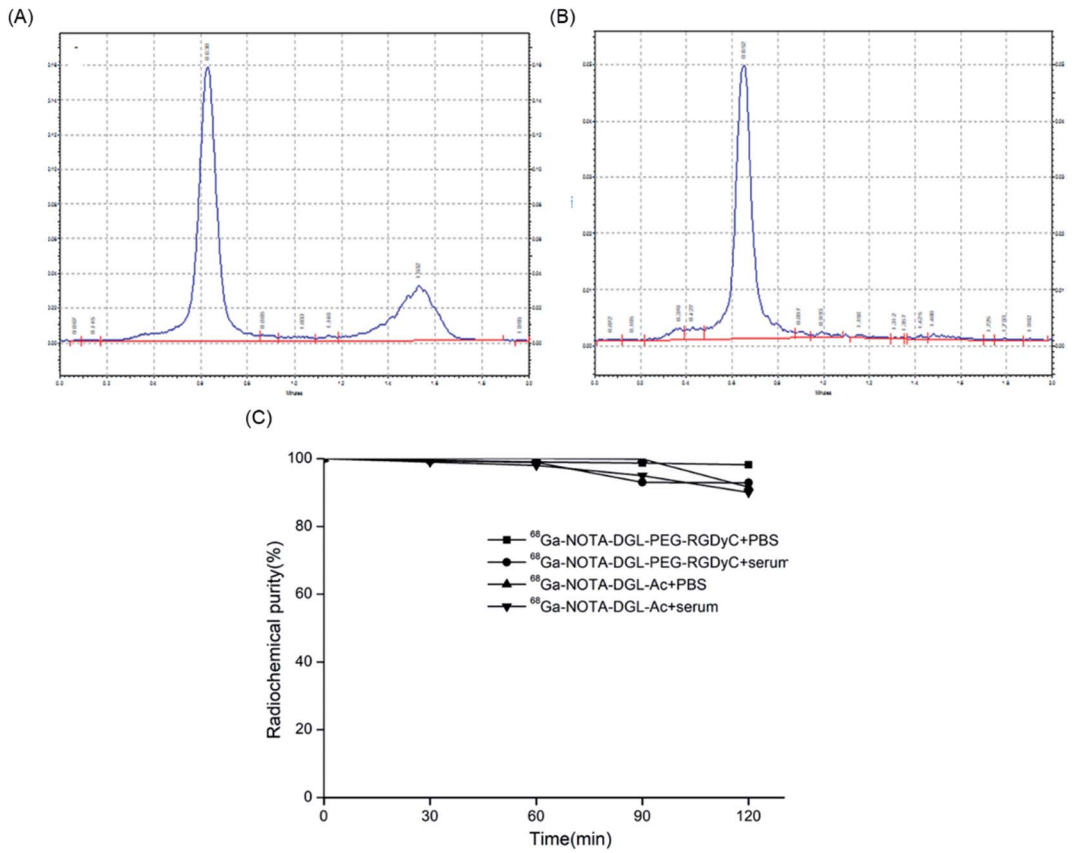

Fig. 3 TLC test results of ^{68}Ga-NOTA-DGL-PEG-RGDyC. Before (A) and after (B) purification by PD10 column. (C) Stability evaluation of ^{68}Ga-NOTA-DGL-PEG-RGDyC and ^{68}Ga-NOTA-DGL-Ac in PBS and serum.

naturally air-dried, the changes in the morphology of red blood cells were observed by scanning electron microscopy (SEM).

3. Results and discussions

3.1. Synthesis and characterization of NOTA-DGL-PEG-RGDyC

As shown in Fig. 1A, RGDyC was conjugated to DGL *via* NHS-PEG-MAL to construct the a nanoprobe carrier, DGL-PEG-RGDyC. In NMR spectra (Fig. 1B), the solvent peak of D_2O was found at 4.7 ppm. The methylene protons of branching units of DGL have multiple peaks between 4.3 and 1.1 ppm. The NMR spectrum of DGL-PEG had a characteristic peak of the MAL group in PEG at 6.2 ppm. The MAL peak disappeared in the NMR spectrum of DGL-PEG-RGDyC, and the repeating unit of PEG still shows a sharp peak at 3.6 ppm, indicating that the MAL group has reacted with the thiol group of RGDyC peptide. The NMR spectrum of DGL-PEG-RGDyC had characteristic peaks of the benzene ring in RGDyC at 6.7 and 7.1 ppm. The NMR spectra result proved the successful synthesis of DGL-PEG-RGDyC.

We further characterized the obtained NOTA-DGL-PEG-RGDyC. UV-Vis spectrum of NOTA-DGL-PEG-RGDyC and NOTA-NHS showed a typical absorption band at around 320 nm, indicating the presence of NOTA in NOTA-DGL-PEG-RGDyC (Fig. 2C).

Next, we used DLS to characterize the size of the prepared NOTA-DGL and NOTA-DGL-PEG-RGDyC (Fig. 2A and B). The results showed that the nanoconjugate exhibits a narrow size distribution. The diameters of NOTA-DGL and NOTA-DGL-PEG-RGDyC were measured to be (35.02 ± 1.53) nm and (139.3 ± 16.9) nm, respectively. The results indicated that NOTA-DGL-PEG-RGDyC was successfully synthesized.

3.2. Quality control tests of ^{68}Ga-NOTA-DGL-PEG-RGDyC

The radiochemical yield of ^{68}Ga-NOTA-DGL-PEG-RGDyC was between 50 and 75%. After separation and purification by PD10 purification column, the radiochemical purity was higher than 98% (Fig. 3B). ^{68}Ga-NOTA-DGL-PEG-RGDyC was a colorless, clear solution with a pH between 4.0 and 4.2. 200 μL of ^{68}Ga-NOTA-DGL-PEG-RGDyC probe was injected into normal nude mice ($n = 3$) through the tail vein for 7 days, and no death of nude mice was observed, indicating that the nanoprobe had no obvious toxicity.

The results of Radio-TLC analysis showed that the retention factor value (R_f value) of $GaCl_3$ was about 1, and the R_f value of ^{68}Ga-NOTA-DGL-PEG-RGDyC was 0.07. The *in vitro* stability study showed that ^{68}Ga-NOTA-DGL-PEG-RGDyC had a radiochemical purity of >95% after standing in 0.01 mol L^{-1} pH 7.4 PBS solution and calf serum for 2 h (Fig. 3C). The above experiments showed that ^{68}Ga-NOTA-DGL-PEG-RGDyC has

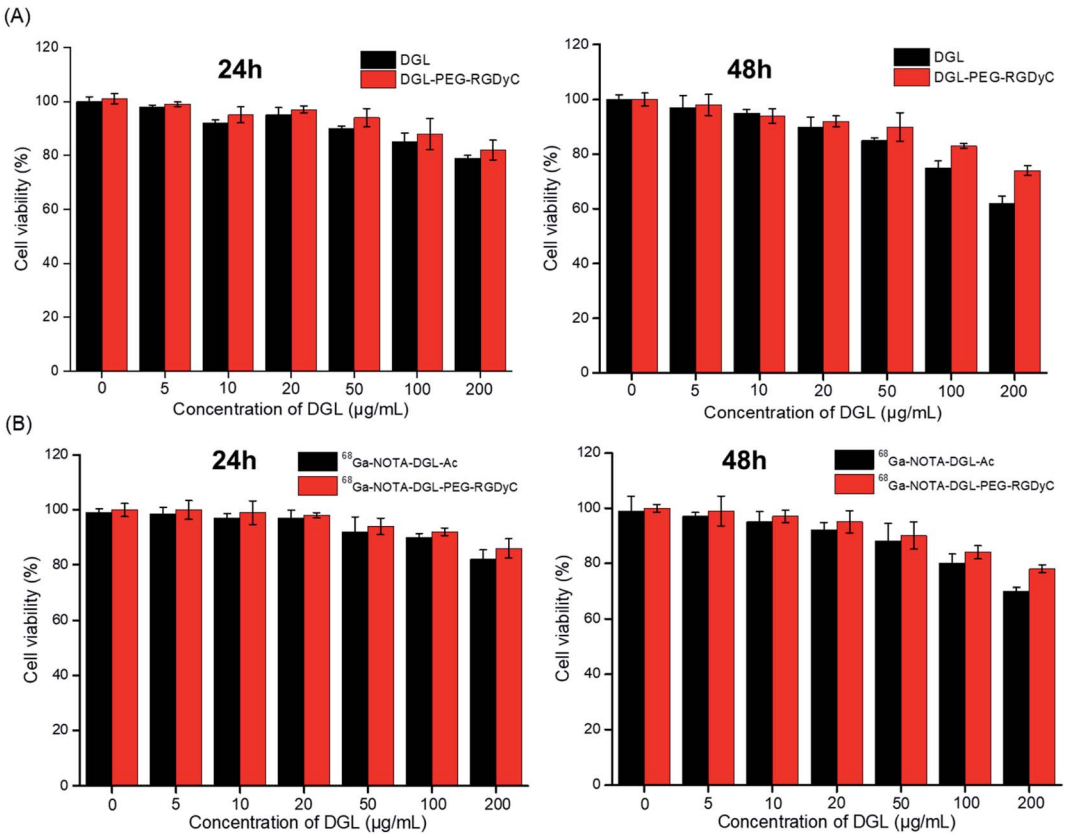

Fig. 4 Percentage viability of U87 cells treated with different complexes (DGL and DGL-PEG-RGDyC(A) or ^{68}Ga-NOTA-DGL-PEG-RGDyC and ^{68}Ga-NOTA-DGL-Ac(B)) at a concentration range from 5 to 200 μg mL^{-1} using CCK-8 assay after 24 h and 48 h incubation at 37 °C.

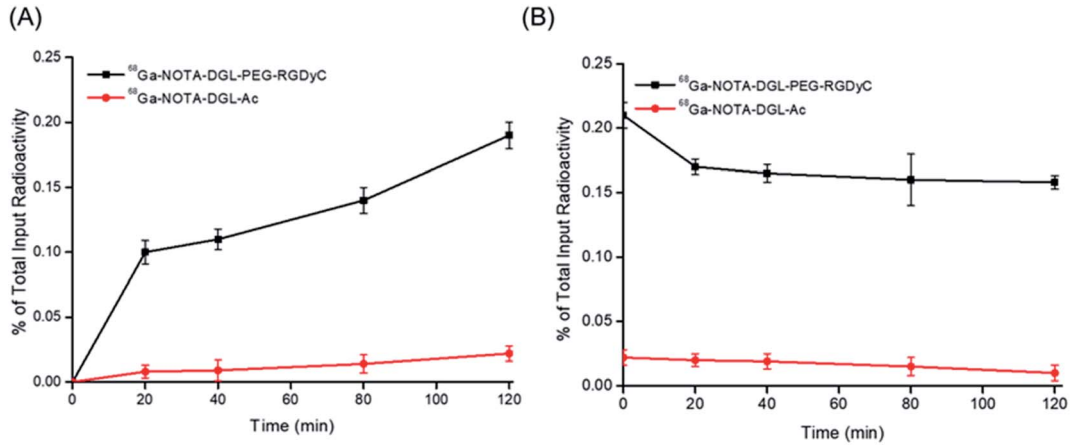

Fig. 5 (A) Radioactivity of ^{68}Ga in U87 cells incubated with ^{68}Ga-NOTA-DGL-PEG-RGDyC and ^{68}Ga-NOTA-DGL-Ac for different times. (B) Elution of ^{68}Ga-NOTA-DGL-PEG-RGDyC and ^{68}Ga-NOTA-DGL-Ac in U87 cells.

excellent *in vitro* stability. The specific activity of the labeled compound was 30 GBq/μmol.

3.3. *In vitro* cytotoxicity assay

The cytotoxicity of different concentrations of NOTA-DGL-PEG-RGDyC nanoparticles on U87MG was detected by CCK-8 method. As shown in Fig. 4A, NOTA-DGL-PEG-RGDyC was relatively low in cytotoxicity after incubation with cells for 24 h or 48 h. When the NOTA-DGL-PEG-RGDyC concentration reached 200 μg mL^{-1}, it showed slight cytotoxicity and the cell viability was about 70%. In addition, the assay results also proved that the ^{68}Ga-NOTA-DGL-PEG-RGDyC probes are not cytotoxic even with a high probe concentration and a prolonged incubation time for U87MG cell lines (Fig. 4B).

3.4. Cell uptake and elution experiments

To determine the cell binding and cell retention characteristics of ^{68}Ga-NOTA-DGL-PEG-RGDyC, U87MG was used for

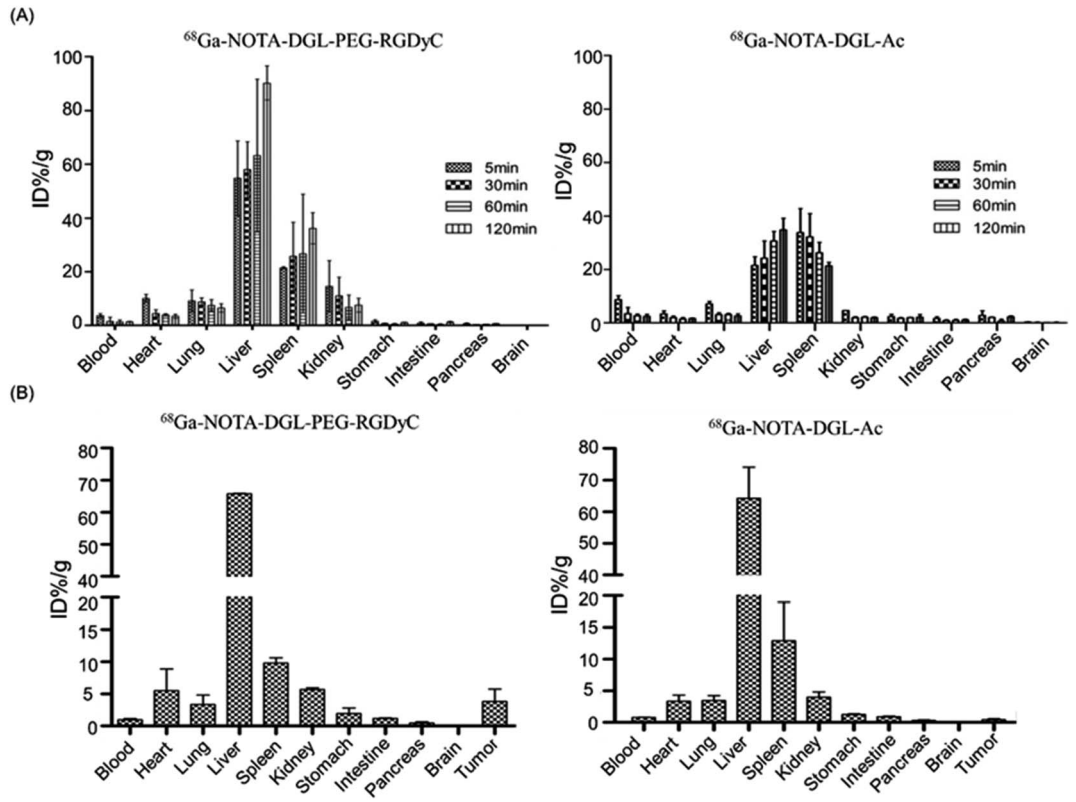

Fig. 6 (A) *In vivo* biology distribution of ^{68}Ga-NOTA-DGL-PEG-RGDyC and ^{68}Ga-NOTA-DGL-Ac in normal mice at four different time intervals (5 min, 30 min, 60 min and 120 min). (B) *In vivo* biology distribution of ^{68}Ga-NOTA-DGL-PEG-RGDyC and ^{68}Ga-NOTA-DGL-Ac in tumor bearing mice at 120 min.

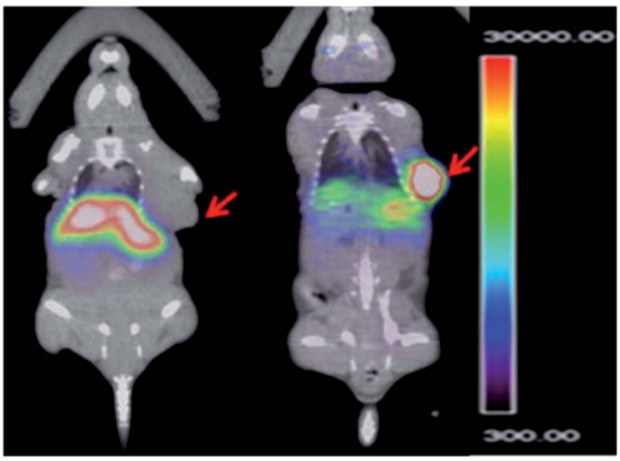

Fig. 7 PET-CT imaging of tumor-bearing nude mice after two hours of tail vein injection.

cell uptake and elution experiments. The ^{68}Ga-NOTA-DGL group served as a negative control group. The results showed that ^{68}Ga-NOTA-DGL-PEG-RGDyC could enter U87MG cells rapidly and efficiently compared with the ^{68}Ga-NOTA-DGL group. As shown in Fig. 5A, and with the prolonged incubation time, the imaging agent further enhanced the cell binding force and reached a peak at 2 h of incubation. The highest cell uptake level of U87MG was 22.7 ± 9.9%, while the ^{68}Ga-NOTA-DGL group showed very low levels of cellular uptake. This demonstrated that RGD did enhance the delivery efficiency of the nanosystem to U87MG cells. In the cell elution experiment, ^{68}Ga-NOTA-DGL-PEG-RGDyC showed a slow decrease in cell length with time. ^{68}Ga-NOTA-DGL-PEG-RGDyC excreted rapidly in U87MG cells for the first 20 minutes, and the cell retention rate decreased from 20.60 ± 1.58% to 16.935 ± 0.88% (Fig. 5B), followed by slow excretion. By the end of 2 hours, the cell retention rate was 16.21 ± 1.31%, indicating that ^{68}Ga-NOTA-DGL-PEG-RGDyC was slowly excreted in the cells.

3.5. Biological distribution

The biodistribution results of ^{68}Ga-NOTA-DGL-PEG-RGDyC and ^{68}Ga-NOTA-DGL-Ac in normal nude mice were shown in Fig. 6A. The results showed that after injection of ^{68}Ga-NOTA-DGL-PEG-RGDyC and ^{68}Ga-NOTA-DGL-Ac, the % ID/g of blood decreased with time. In particular, 5 min after injection and 30 min after injection were significantly different, each being (3.64 ± 0.52), (1.52 ± 1.27) and (8.73 ± 1.21), (3.43 ± 1.93)% ID/g, indicating ^{68}Ga-NOTA-DGL-PEG-RGDyC and ^{68}Ga-NOTA-DGL-Ac cleared faster in the first 30 min of blood and then slowed down. The radioactivity uptake in the liver and spleen increased with time, and the renal uptake was lower at each time point, indicating that ^{68}Ga-NOTA-DGL-PEG-RGDyC and ^{68}Ga-NOTA-DGL-Ac were mainly affected by Liver and spleen RES system phagocytosis.

We further evaluated the biodistribution of ^{68}Ga-NOTA-DGL-PEG-RGDyC and ^{68}Ga-NOTA-DGL-Ac in tumor-bearing nude mice. Briefly, the nanomolecular probe ^{68}Ga-NOTA-DGL-PEG-RGDyC was injected into nude mice by tail vein injection. After 2 hours, the degree of radioactivity absorption of tumor tissues and major organs is shown in Fig. 6B. The uptake values of liver, spleen and tumor tissues were (64.27 ± 8.00)% ID/g, (12.90 ± 4.95)% ID/g and (4.67 ± 0.09)% ID/g, respectively. The results showed that ^{68}Ga-NOTA-DGL-PEG-RGDyC was mainly phagocytized by RES system such as liver and spleen. Due to the targeting effect of RGD, it was also distributed in tumor sites.

3.6. Positron emission tomography (PET) imaging of tumor bearing mice

The targeting ability of ^{68}Ga-NOTA-DGL-PEG-RGDyC was evaluated by PET imaging experiments. The result was shown in Fig. 7. Compared to untargeted ^{68}Ga-NOTA-DGL-Ac, RGD-modified ^{68}Ga-NOTA-DGL-PEG-RGDyC showed significant PET signal at the tumor site after 2 h of intravenous injection. The results of this experiment indicated that the modification of RGD enhanced the material's targeting to tumors.

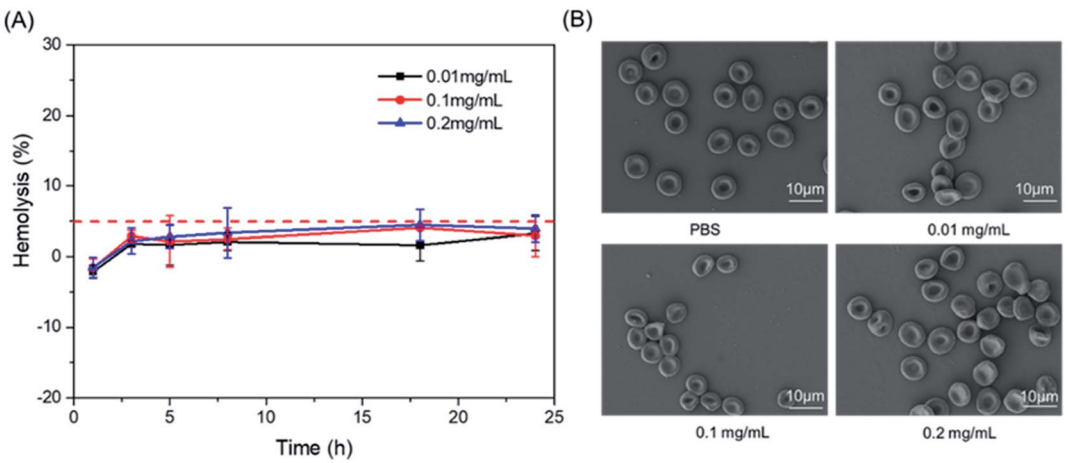

Fig. 8 Effect of NOTA-DGL-PEG-RGDyC with different concentrations on the hemolysis (A) and the aggregation and morphology of RBCs (B).

3.7. Blood compatibility

The blood compatibility of NOTA-DGL-PEG-RGDyC was investigated by hemolysis test and morphological changes of red blood cells. As shown in Fig. 8A, 0.2 mg mL^{-1} NOTA-DGL-PEG-RGDyC did not cause hemolysis (the hemolysis rate below 5%).[35] In addition, the effect of NOTA-DGL-PEG-RGDyC on red blood cells was further evaluated. As shown in Fig. 8B, it was further confirmed that NOTA-DGL-PEG-RGDyC has good blood biocompatibility. The results showed that NOTA-DGL-PEG-RGDyC had no significant effect on the morphology of red blood cells in the concentration range of 0.01–0.2 mg mL^{-1}.

4. Conclusion

In this study, the NOTA-DGL-PEG-RGDyC precursor was successfully synthesized on the basis of NOTA-DGL, and the target product ^{68}Ga-NOTA-DGL-PEG-RGDyC was obtained by ^{68}Ga labeling. The method has short reaction time, simple steps and high radiochemical yield. After purification by PD10 column, the radiochemical purity was more than 95% and the stability *in vitro* was good. Compared with the untargeted nanoprobe ^{68}Ga-NOTA-DGL-Ac, it was demonstrated that the targeted nanoprobe ^{68}Ga-NOTA-DGL-PEG-RGDyC has a certain active target for U87MG glioma cells in the cell uptake and elution experiments. The distribution experiments in normal mice showed that the nano-probes ^{68}Ga-NOTA-DGL-PEG-RGDyC and ^{68}Ga-NOTA-DGL-Ac cleared faster in the blood, and the imaging agents mainly concentrated in the liver. *In vivo* biodistribution experiments in U87MG tumor-bearing mice and Micro-PET imaging in U87MG tumor-bearing mice showed that ^{68}Ga-NOTA-DGL-PEG-RGDyC could be enriched in tumor tissue, which is the future intratumoral radioactivity treatment provides research basis.

Conflicts of interest

No competing financial interests exist.

Acknowledgements

This study was supported financially by the Natural Science Foundation of China (No. 81571733 and 81272105), the Science and Technology Program of Guangzhou (201508020253, 201508020115, 201604020094, 201601010270, 2017010160489, 201704030083, 201907010032, 201907010037), and the Joint Logistic Support Force Project (CWH17J023).

References

1 W. T. Yang, M. Suen, A. Ahuja and C. Metreweli, *Br. J. Radiol.*, 1997, **70**, 685–690.
2 R. Popovtzer, A. Agrawal, N. A. Kotov, A. Popovtzer, J. Balter, T. E. Carey and R. Kopelman, *Nano Lett.*, 2008, **8**, 4593–4596.
3 S. Zhao, X. Yu, Y. Qian, W. Chen and J. Shen, *Theranostics*, 2020, **10**, 6278–6309.
4 K. Kitajima, K. Murakami, E. Yamasaki, I. Fukasawa, N. Inaba, Y. Kaji and K. Sugimura, *Am. J. Roentgenol.*, 2008, **190**, 1652–1658.
5 F. Vos, C. Bleeker-Rovers, F. Corstens, B. Kullberg and W. Oyen, *Q. J. Nucl. Med. Mol. Imag.*, 2006, **50**, 121.
6 S. Yasuda and M. Ide, *Ann. Nucl. Med.*, 2005, **19**, 167–177.
7 V. Ambrosini, D. Campana, P. Tomassetti, G. Grassetto, D. Rubello and S. Fanti, *Eur. J. Radiol.*, 2011, **80**, e116–e119.
8 H. R. Maecke, M. Hofmann and U. Haberkorn, *J. Nucl. Med.*, 2005, **46**, 172S.
9 M. Sathekge, *Nucl. Med. Commun.*, 2008, **29**, 663–665.
10 V. Ambrosini, P. Tomassetti, P. Castellucci, D. Campana, G. Montini, D. Rubello, C. Nanni, A. Rizzello, R. Franchi and S. Fanti, *Eur. J. Nucl. Med. Mol. Imag.*, 2008, **35**, 1431–1438.
11 O. Alonso, M. Rodríguez-Taroco, E. Savio, C. Bentancourt, J. P. Gambini and H. Engler, *Ann. Nucl. Med.*, 2014, **28**, 638–645.
12 L. Wei, Y. Miao, F. Gallazzi, T. P. Quinn, M. J. Welch, A. L. Vāvere and J. S. Lewis, *Nucl. Med. Biol.*, 2007, **34**, 945–953.
13 E. Borges, Y. Jan and E. Ruoslahti, *J. Biol. Chem.*, 2000, **275**, 39867–39873.
14 J. Li, X. Zhang, M. Wang, X. Li, H. Mu, A. Wang, W. Liu, Y. Li, Z. Wu and K. Sun, *Int. J. Pharm.*, 2016, S0378517316300680.
15 Y. H. Kim, J. Jeon, H. H. Su, W. K. Rhim, Y. S. Lee, H. Youn, J. K. Chung, M. C. Lee, S. L. Dong and K. W. Kang, *Small*, 2011, **7**, 2052–2060.
16 Y. Yang, L. Zhang and C. Zhang, *Nanomed. Nanotechnol. Biol. Med.*, 2016, **12**, 525.
17 U. Prabhakar, H. Maeda, R. K. Jain, E. M. Sevick-Muraca, W. Zamboni, O. C. Farokhzad, S. T. Barry, A. Gabizon, P. Grodzinski and D. C. Blakey, *AACR*, 2013, vol. 7, p. 472.
18 J. Yuan, Y. You, X. Lu, O. Muzik, D. Oupicky and F. Peng, *Mol. Imaging*, 2007, **6**, 7290.2006.00030.
19 M. Breunig, U. Lungwitz, R. Liebl and A. Goepferich, *Proc. Natl. Acad. Sci. U.S.A.*, 2007, **104**, 14454–14459.
20 D. J. Bharali, M. Khalil, M. Gurbuz, T. M. Simone and S. A. Mousa, *Int. J. Nanomed.*, 2009, **4**, 1.
21 K. Greish, in *Cancer Nanotechnology*, Springer, 2010, vol. 31. pp. 25–37.
22 D. A. Tomalia and J. M. Fréchet, *J. Polym. Sci., Part A: Polym. Chem.*, 2002, **40**, 2719–2728.
23 Y. Kodama, H. Kuramoto, Y. Mieda, T. Muro, H. Nakagawa, T. Kurosaki, M. Sakaguchi, T. Nakamura, T. Kitahara and H. Sasaki, *J. Drug Target.*, 2017, **25**, 49–57.
24 F. Oukacine, B. Romestand, D. M. Goodall, G. Massiera, L. Garrelly and H. Cottet, *Anal. Chem.*, 2012, **84**, 3302–3310.
25 B. Romestand, J.-L. Rolland, A. Commeyras, G. Coussot, I. Desvignes, R. Pascal and O. Vandenabeele-Trambouze, *Biomacromolecules*, 2010, **11**, 1169–1173.
26 P. B. Alexander and X.-F. Wang, *Front. Med.*, 2015, **9**, 134–138.
27 T. Zou, F. Oukacine, T. Le Saux and H. Cottet, *Anal. Chem.*, 2010, **82**, 7362–7368.
28 L. E. Prevette, D. G. Mullen and M. M. Banaszak Holl, *Mol. Pharm.*, 2010, **7**, 870–883.

29 J. Li, S. Huang, K. Shao, Y. Liu, S. An, Y. Kuang, Y. Guo, H. Ma, X. Wang and C. Jiang, *Sci. Rep.*, 2013, **3**, 1623.
30 R. Li, F. Jiang, Q. Xiao, J. Li, X. Liu, Q. Yu, Y. Liu and C. Zeng, *Nanotechnology*, 2010, **21**, 475102.
31 Q. Wang, J. Li, S. An, Y. Chen, C. Jiang and X. Wang, *Int. J. Nanomed.*, 2015, **10**, 4479.
32 G. Hu, H. Zhang, L. Zhang, S. Ruan, Q. He and H. Gao, *Int. J. Pharm.*, 2015, **496**, 1057–1068.
33 Y. Wang, Z. Miao, G. Ren, Y. Xu and Z. Cheng, *Chem. Commun.*, 2014, **50**, 12832–12835.
34 D. Zhong, Y. Jiao, Y. Zhang, W. Zhang, N. Li, Q. Zuo, Q. Wang, W. Xue and Z. Liu, *Biomaterials*, 2013, **34**, 294–305.
35 Z. Li, J. Shao, Q. Luo, X.-F. Yu, H. Xie, H. Fu, S. Tang, H. Wang, G. Han and P. K. Chu, *Biomaterials*, 2017, **133**, 37–48.